Recent Progress in Modeling the Plasmasphere, Energetic Particles, as well as the Interaction between the Solar Wind and the Magnetosphere

Joseph Lemaire[1] - Viviane Pierrard[1] - Marius Echim[4] - Tsvetan Dachev[3] - Mathias Cyamukungu[2] - Ghislain Grégoire[2]

jl@oma.be

[1]**BIRA-IASB & ASTR-UCL,**
Avenue Circulaire, 3
Bruxelles, 1180, Belgium

[2] **CSR, FYNU-UCL,**
Chemin du Cyclotron, 2,
Louvain-la-Neuve, 1348, Belgium

[3] **STIL-BAS, Acad. G.**
Bonchev Str. Block 3,
Sofia, Bulgaria

[4]**ISS,**
Atomistilor, 1,
P.O. Box MG-23,
R-76900 Margurelle
Bucharest, Roumania

ABSTRACT

This paper reports additional activities of the Center for Space Radiation (CSR) at the Institut de Physique Nucléaire of the Université Catholique de Louvain, and, of the Belgian Institute for Space Aeronomy (IASB-BIRA) in the field of magnetospheric physics not presented in the companion paper of this volume. It outlines recent theoretical contributions on the distribution of thermal particles in the Plasmasphere as well as on their convective stability. The electron density profiles deduced from the ISEE-2 wave experiment have been used as a baseline in this study. This paper addresses also the progress made in simulating the mechanism of Impulsive Penetration of solar wind plasma elements into the magnetosphere. Finally, we outline the results that have been obtained about the distribution of energetic protons trapped in the geomagnetic field during highly disturbed geomagnetic conditions. For this purpose we have used the energetic particle fluxes measured with the Charged Particle Telescope (CPT) onboard the Danish satellite OERSTED, as well as with the LIULIN fluxmeter and dosimeter which operated for 3 years on board of the MIR station. The results of these two sets of observations are summarized in the third part of this paper.

KEYWORDS

Plasmasphere; Magnetopause; Impulsive Penetration; Radiation Belt; High Energy Electrons and Protons

THE PLASMASPHERE

Since 1974 there has been continuing interest at IASB in modeling the physical process leading to the formation of the plasmapause, and in modeling the deformation of the plasmasphere during disturbed space weather conditions. The contributions in this field have been reported in a book published at Cambridge University Press by Lemaire and Gringauz (1998). It is a comprehensive review of all relevant observations of the plasmasphere until about 1996. Besides the theoretical modeling efforts in this area, this book reports also the historical discovery of the plasmapause based on observations of the Soviet LUNIK-1&2 interplanetary spacecraft, as well as on whistler observations by Carpenter in the USA.

Our recent contributions in this field of investigations since 1994, are focussed on the following topics: a) the formation of plasmatails attached to the plasmasphere during a sudden enhancement of the magnetospheric electric field; b) a comparison of different models of density distributions in the plasmasphere based on non-maxwellian and non-isotropic velocity distributions of thermal H^+-ions and electrons along dipole magnetic field lines; c) these theoretical models are then compared with observations of the electron density obtained during the ISEE-2 mission; d) finally, their convective stability with respect to interchange and quasi-interchange have been examined.

Formation of plasmatails

The relative abundance of Helium in the plasmasphere has become a hot topic in magnetospheric physics due to the forthcoming results of the IMAGE mission. In this perspective Reynolds et al. (1999) have developed a kinetic exospheric model to calculate the densities of Helium ions and Hydrogen ions in the equatorial region of the plasmasphere. The convection velocity of plasmaspheric flux tubes in their model is based on McIlwain's electric field model, E5H, which is also used by Lemaire (2000) in his simulation of the formation of plasmatails.

Figure 1 shows the deformation of the equatorial cross-section of the plasmasphere due to an enhancement of the dawn-dusk component of the magnetospheric electric field when Space Weather conditions suddenly become active as indicated in the top panel by the significant increase of the value of the K_p geomagnetic index. It can be seen how a plasmatail is formed in the post-noon local time sector as a consequence of the development of a bulge in the pre-noon sector due to the enhanced value of dawn-dusk component of the electric field and to the resulting enhanced sunward convection velocity; as a consequence of the differential azimuthal, convection velocity this dayside bulge corotates into the post-noon sector with a smaller angular speed at large radial distances than closer to Earth. This differential angular velocity inherent in the Kp-dependent E5H electric field model, produces the tail-like structure shown in the last panels of figure 1. This mechanism for the formation of plasmatails attached to the plasmasphere in the dusk sector was proposed by Lemaire (2000). It is an alternative mechanism to the sunward surging of the outermost plasmasphere shell that takes place in the dusk region, and proposed in the 80's to produce similar plasmatails in the pre-dusk sector. The new scenario illustrated in figure 1 has been simulated numerically by Lemaire (2000).

The preliminary observations using the EUV mapping of He^+ in the plasmasphere becoming now available from the IMAGE mission will enable us to test the validity of both mechanisms proposed for the formation of plasmatails attached to the central core of the plasmasphere, including that illustrated in figure 1.

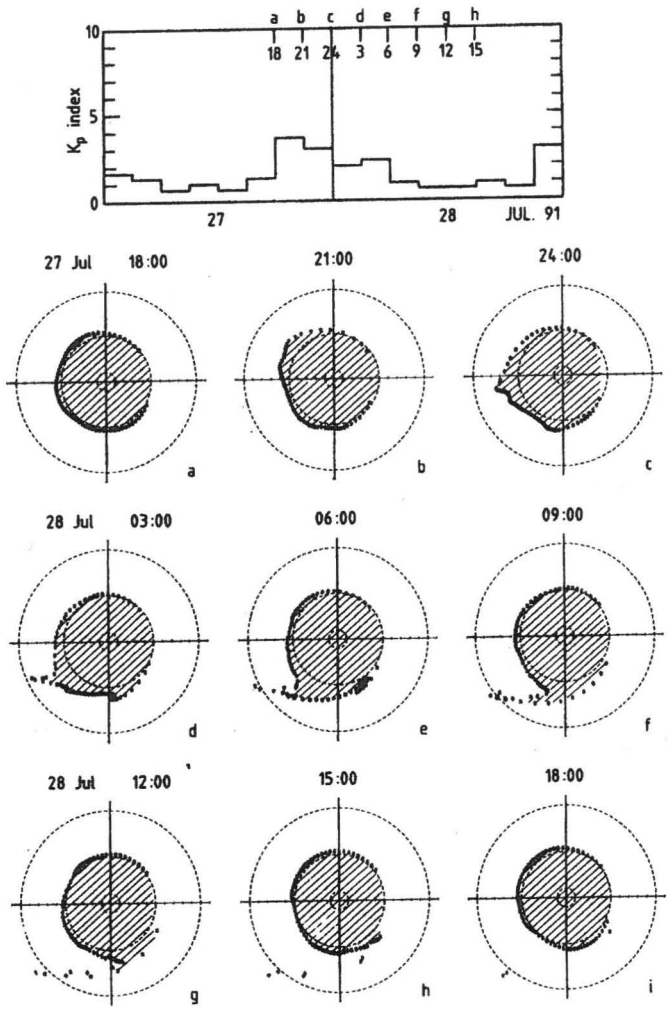

Figure 1: Formation of plasmaspheric tails due to enhanced magnetospheric convection and differential angular velocity (Lemaire, 2000)

Field-aligned density and temperature profiles in the plasmasphere

The field-aligned density distribution of ionospheric plasma along dipole magnetic field lines depends on the assumed/postulated Velocity Distribution Function (VDF) and Pitch Angle Distribution (PAD) of the electrons and ions at a given reference altitude (h_o) in the topside ionosphere. In the past, maxwellian VDF and isotropic PAD were generally assumed to model the field-aligned density profiles in the plasmasphere. This leads to a plasmasphere in hydrostatic or barometric equilibrium with no field-aligned flow of ionization. In such maxwellian barometric models the ion and electron densities are determined by

$$n(L,\lambda) = n_o(L,\lambda_o)\exp\left[-m_H\psi(L,\lambda)/k(T_{o,e}+T_{o,p})\right] \qquad (1)$$

where $n_o(L,\lambda_o)$ is the electron density or proton density at the reference altitude h_o, and at the latitude λ_o along the magnetic field line determined by McIlwain's parameter L; $T_{o,e}(L, \lambda_o)$ and $T_{o,p}(L, \lambda_o)$ are respectively the electron and proton temperatures at the reference altitude; in this expression the total potential of the electrons or protons is determined by

$$\psi(r) = \phi_g(r) - \frac{1}{2}\Omega^2 r^2 \cos\lambda \qquad (2)$$

where ϕ_g is the gravitational potential; and Ω is the angular velocity of exospheric plasma. As a consequence of the large field-aligned electrical conductivity, the ion-exosphere is strongly coupled to the corotating ionosphere; therefore the angular velocity of the plasmasphere tends to be equal to that of the ionosphere of the Earth: $\Omega = \Omega_E$,.

When the VDF of the electrons and protons is isotropic and maxwellian, the field aligned distribution of the temperature, $T(L,\lambda)$, of the electrons and protons is independent of altitude, and equal to $T_{o,e}$ and $T_{o,p}$, respectively. The temperature is then also independent of the equatorial radial distance, provided that the exobase temperature $T_o(L,\lambda_o)$ does not depend on the latitude λ_o where the field lines traverse the surface of the reference level.

The field aligned density is different from that given by (1) when the VDF is non-maxwellian, but for instance has an enhanced tail of suprathermal particles with a power law energy spectrum $\left[: \left(\frac{mv^2}{2kT} \right)^{-\kappa} \right]$ corresponding to a lorentzian VDF, instead of the exponential energy spectrum $\left[: \exp\left(-\frac{mv^2}{2kT} \right) \right]$ corresponding to a maxwellian VDF. Pierrard and Lemaire (1996b-98) have shown that when the VDF is lorentzian and isotropic, the hydrostatic/barometric density distribution decreases more slowly with altitude. The field-aligned density and temperature distributions are then given by

$$n(L,\lambda) = n(L,\lambda_o)\left[1 + \frac{m_H \psi(L,\lambda}{\kappa k (T_{o,e} + T_{o,p})} \right]^{-\kappa+1/2} \tag{3}$$

$$T(L,\lambda) = T_o(L,\lambda_o)\frac{\kappa}{\kappa - 3/2}\left[1 + \frac{m_H \psi(L,\lambda)}{\kappa k (T_{o,e} + T_{o,p})} \right] \tag{4}$$

It has been shown by Pierrard and Lemaire (1996) that when $\kappa \to \infty$ (i.e. when the lorentzian VDF tends asymptotically to the corresponding maxwellian VDF) the expression (3) tends asymptotically to (1). The temperature tends then to become independent of altitude as in a maxwellian barometric model. In such a lorentzian model, the temperature (4) increases with altitude along magnetic field lines when $\psi(r)$ is an increasing function of altitude. Such a positive temperature gradient is supported by observations. Indeed, the ion temperature measurements made by PROGNOZ, PROGNOZ-2 as well as DE-1 satellites have shown that the ion temperature increases with altitude in the outermost flux tubes of the plasmasphere and of the plasmatrough (Gringauz and Bezrukikh, 1976; Gringauz, 1985; Comfort et al., 1985). Several alternative theories have already been proposed to explain the observed positive temperature gradients in the terrestrial plasmasphere: e.g. heating of the upper layers of the plasmasphere by wave-particle interactions whose energy is supplied by Ring Current ions (Kozyra *et al.*, 1987) or by photoelectrons (Horwitz *et al.*, 1990; Comfort, 1996).

Without rejecting these different alternative mechanisms and theories, Pierrard and Lemaire (1996) propose that part of the positive temperature gradient observed in the topside ionosphere can be accounted for by the departure of the VDF from the usual maxwellian one: i.e. by an enrichment of the population of suprathermal ions in the VDF. Such an enrichment of the suprathermal particle population may be the result of the velocity filtration effect of Coulomb collisions whose cross section decreases as the fourth inverse power of the relative velocity of the colliding particles. This velocity filtration effect has first been proposed by Scudder (1992a,b) to explain the similar positive temperature gradient in the solar corona.

Equatorial density distributions profiles

Eqs. (1) and (3) have been used by Lemaire (1999) to calculate the distribution of density in the equatorial plane (i.e. for $\lambda = 0$) as a function of radial distance L. The dotted-dashed line in figure 2 corresponds to the equatorial density profile for a lorentzian VDF with $\kappa = 4$, when the angular rotation speed (Ω) of the protonosphere is equal to zero. The electron and proton temperatures and densities at the exobase level are assumed to be independent of the invariant latitude λ_o and both equal to $T_{oe} = T_{op} = 4000$ K; $n_{oe} = n_{op} = 3890$ cm^{-3}. It can be seen that the density tends asymptotically to a constant at large equatorial distances and that the density scale height increases continuously to become infinitely large at $L = \infty$.

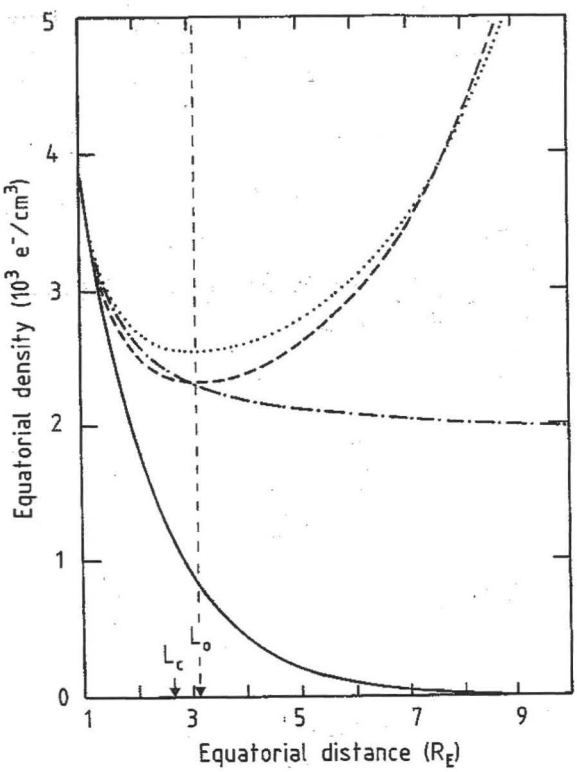

Figure 2: Equatorial plasma density distribution observed by Carpenter and Anderson (1992) (:solid line); dashed-dotted curve corresponds to the electron density profile for a non-rotating protonosphere in hydrostatic/barometric equilibrium and when the velocity distribution function is a κ=4 lorentzian function; dotted curve corresponds to the same model but for an angular velocity equal to 3 times the angular rotation speed of the Earth; the dashed curve corresponds to a rotating ($\Omega = 3\Omega_E$) protonosphere with a maxwellian velocity distribution function (Lemaire, 1999).

The dotted line is obtained for the same lorentzian VDF ($\kappa = 4$) and for the same exobase boundary conditions, but corresponds to an angular rotational speed equal to three times that of the Earth. Large azimuthal velocities are indeed expected in the distant nightside plasmasphere during intense substorm enhancements of the magnetospheric convection velocity. Due to the centrifugal effect the equatorial density distribution has a minimum value at $L = L_o = 3.17$, where the radial components of gravitational and centrifugal force balance each other. At this equatorial distance the density scale height is equal to ∞. Beyond this distance the equilibrium hydrostatic/barometric density distribution increases indefinitely with L. Any negative density slope in such background protonosphere model would be convectively unstable as shown below.

The dashed line in figure 2 corresponds to a maxwellian isotropic VDF and an angular velocity of $3\Omega_E$. It can be seen that the minimum density is again located at $L = L_o = 3.17$ but is lower than in the corresponding lorentzian case (dotted line). It is important to note that the equatorial distance of the minimum in the hydrostatic/barometric density profile does not depend on the index κ characterizing the VDF (Lemaire,1999).

The solid line in figure 2 is a fit to the observed electron density profile obtained by Carpenter and Anderson (1992) using plasma wave measurements along the orbit of the ISEE spacecraft. This equatorial density profile has been measured in the magnetosphere close to the equatorial plane after an extended period of quiet conditions. The density scale height associated with this equatorial profile is equal to 1.38 R_E and is almost independent of L. Note that the density distribution has no minimum value at $L = 6.6$ as expected if the protonosphere would be in hydrostatic/barometric equilibrium and rotating with the angular speed of the Earth. This property of the observed equatorial plasma density profile (solid line in figure 2) leads to the following conclusions: the pitch angle distribution of the thermal ions cannot be isotropic if the plasmasphere would be in hydrostatic equilibrium (i.e. in the absence of any plasmaspheric wind expansion): i.e. the trapped, ballistic, escaping and incoming particles cannot be in detailed balance equilibrium. Pierrard and Lemaire (2001) have determined the relative fraction of trapped particles that are needed in addition of ballistic, escaping and incoming ones, in order to obtain the observed equatorial density distribution shown by the solid line in figure 2. They found that the fraction of trapped particles with pitch angles outside the source and loss cones, and, mirror points above the reference altitude must be a decreasing function of L or λ_o. This function was calculated in Pierrard and Lemaire's (2001) hydrostatic/exospheric model. They find that along magnetic field lines with increasing L-values, the equatorial pitch angle distribution (PAD) of thermal ions gets more and more depleted of trapped particles with equatorial pitch angles close to 90°, i.e. particles with mirror points close to the equatorial plane are missing. For increasing L, the PAD tends to become more cigar-like, with larger fluxes in the field-aligned direction than in the direction perpendicular to the magnetic field; for smaller values of L the PAD tends to be more isotropic. This important result should be tested using low energy (< 1 eV) ion directional flux measurements. Unfortunately, reliable directional observations at such low energies are not yet available due to spacecraft charging effects.

SIMULATION OF THE IMPULSIVE PENETRATION OF SOLAR WIND IN THE MAGNETOSPHERE

The solar wind and magnetosheath plasmas are non-uniform. Their density and momentum density are not uniformly distributed over the magnetopause surface. This has lead Lemaire (1977) and Lemaire and Roth (1978) to propose the theory of Impulsive Penetration (IP) of solar wind/magnetosheath plasma filaments or blobs into the magnetosphere. They are stopped and dissolve in the magnetopause boundary layer separating the low density and energetic magnetospheric plasma from the colder and denser magnetosheath plasma of solar wind origin. A review of this non-stationary interaction mechanism between the magnetosphere and the solar wind has been published by Lemaire and Roth (1991).

More recently an update review on this topic has been published in Space Science Review by Echim and Lemaire (2000). In this article the authors review more specifically the different Laboratory experiments and numerical simulations of the IP mechanism. This exercise has lead the authors to calculate the trajectories of charged particles across sheared magnetic field distributions corresponding to different classes of tangential discontinuities. They applied their calculation to the penetration of magnetosheath protons and electrons convected across the magnetopause surface that they approximated by a planar collisionless tangential discontinuity perpendicular to the ox-axis. Various distributions of the convection electric fields have been assumed by Echim and Lemaire (2001). This study was restricted to inhomogeneous B-fields and E-fields distributions perpendicular to the ox axis: i.e. B and E have no component parallel to ox but their y and z components are arbitrarily chosen functions of the x coordinate that is normal to the magnetopause.

The result of their calculation is shown in figure 3. The various panels show the projections on the (x, y) and (x, z) planes of the magnetic and electric field components as a function of x; the trajectory of a proton is also shown; in the case illustrated here the Larmor gyroradius (r_L) is significantly smaller than (L) the scale length over which these fields change. Since the Alfvèn condition ($r_L/L << 1$) for both the magnetic

and electric field is satisfied, the guiding center approximation is applicable to describe the motion of the particle. This approximation can then be used to calculate the phase averaged position of the drifting protons or electrons. This mean location of the particle averaged over a gyroperiod is shown by the dashed lines in figs. 3, c, d, while the independently calculated guiding center positions are given by dashed lines. The good fit between these two curves is a consequence of the smallness of r_L / L .

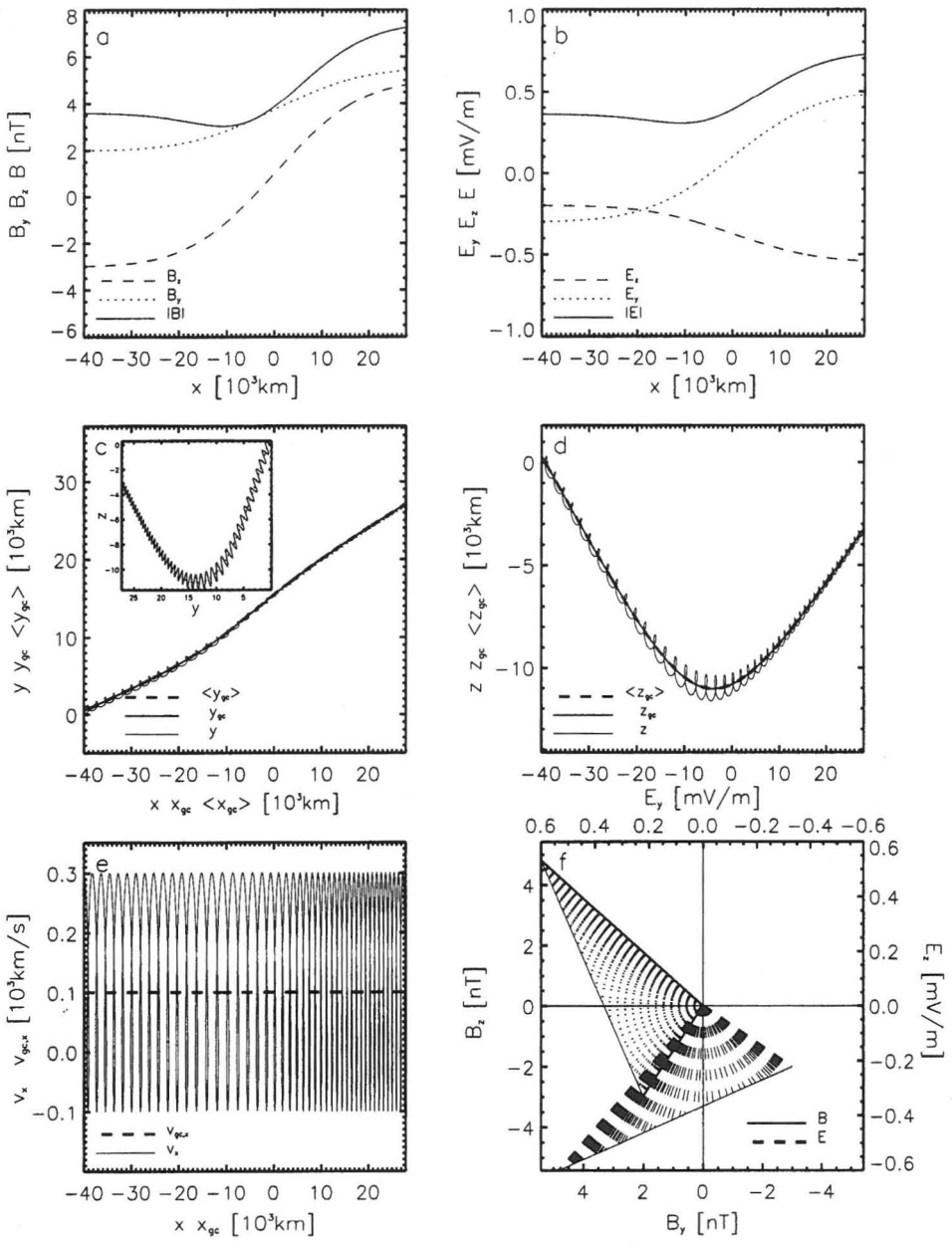

Figure 3: Distributions of the magnetic and electric field components (panels a, b &f) as a function of the distance (x) perpendicular to the tangential discontinuity (TD). Panels c & d show the trajectory of an ion drifting across the TD (thin solid line); the guiding center path is shown by the thick solid line; the dashed line in each panel is the mean position phase-averaged over the local gyro period; panel e shows the ox component of the particle velocity (thin solid line) and guiding center (dashed line) (Echim and Lemaire, 2001).

Echim and Lemaire (2001) have shown that when the Alfvèn conditions are not satisfied, the calculated drift path of the guiding center differs significantly from that of the phase averaged position of the particle.

Furthermore, it has been shown that the magnetic moment of the particle is not adiabatically conserved when the Alfvèn condition is not satisfied.
Echim and Lemaire (2001) have shown also that the electric field distribution generally assumed in 2-D reconnection models, is not the exclusive one. For instance, there is an alternative electric field distribution for which ExB/B^2, the electric drift velocity perpendicular to the magnetopause, is independent of x. They determined also the motion of particles in cases for which the E-field model was designed in such a way that the magnetic moment of the particle is conserved while it drifts across the magnetopause.
All these calculations confirm that the Alfvèn condition is generally not satisfied for suprathermal protons of the solar wind with thermal velocities larger than 100 km/s, or electrons with energies larger than 100 keV. At the magnetopause, under such conditions, their penetration into the magnetosphere can by no means be described in the framework of the first order guiding center approximation.

RADIATION BELT PARTICLE MEASUREMENTS

Model comparison

The distribution of energetic protons and electrons in the Earth's magnetosphere has been modeled by NASA in the 60's and 70's. The results of this long term effort are the AP-8-MIN, AP-8-MAX, AE-8-MIN and AE-8-MAX empirical/statistical Radiation Belt models. These models still remain standards and references within the magnetospheric modeling community. The models used in Russia have been developed at the Institute for Nuclear Physics (INP) of the Moscow State University (MSU). A comprehensive comparison between these INP/MSU statistical models and the corresponding NASA models has been undertaken and published by Beliaev and Lemaire (1996).

Figure 4 illustrates as a function of L, the differences between the equatorial energy spectras of trapped protons in both models. The isocontours determine the AP-8-MIN energy spectrum of protons in the range $0,1 < E < 1000$ MeV, in the equatorial plane as a function of L, for $1 < L < 6.5$. In the domains where the color is white both models predict the same fluxes; where it is reddish the flux of the INP/MSU model is higher than that of the NASA model. Where the color is blue the NASA models predicts higher fluxes than the Russian ones. For L-values or energies outside the ranges of validity of both models, the color is grey. This new graphical method of displaying differences between two similar model quantities has been applied by Beliaev and Lemaire (1994) to other plots where the fluxes are given in (B,L) or (B,E) coordinates.

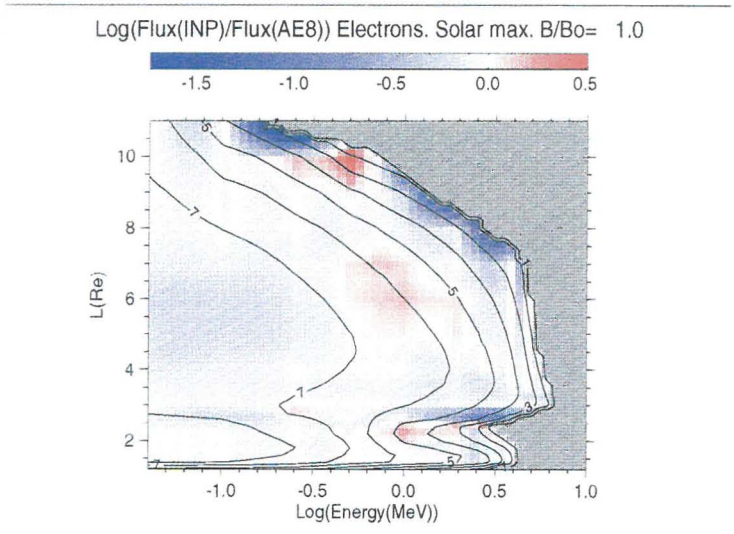

Figure 4: Omnidirectional energy spectrum of trapped energetic electrons (horizontal logarithmic scale in MeV) for different equatorial distances (L in Earth radii: vertical scale). The solid lines are iso-flux contours corresponding to the average static AE-8 Radiation belt model developed in the 60-70's at NASA. The blue color (see color scale) indicates the domains in the (E,L) coordinates where the electron flux of the American model exceeds the corresponding flux of the Russian model (INP) developed at the Institute for Nuclear Physics of the Moscow State University. Where the color is red the flux of the INP model is larger than that of AE-8-MAX (Beliaev and Lemaire, 1994).

The energy spectra of Van Allen belt particles are often fitted by power law distributions. Pierrard and Lemaire (1996a) have shown that the sum of two maxwellian functions is a better fit function for the energy spectra of the AE-8 model. This study indicates that there are two different populations of trapped electrons with significantly different thermal speeds (i.e. characteristic temperatures). The ratio of the soft electron population and more energetic population (hard electrons) changes continuously with L from the inner to the outer Radiation Zones. Figure 5 illustrates the equatorial profiles of the densities (a) and mean energy (b) respectively for the soft electrons (squares) and hard electrons (circles), as a function of L. The solid and open symbols correspond to the AE-8-MIN and AE-8-MAX models respectively.

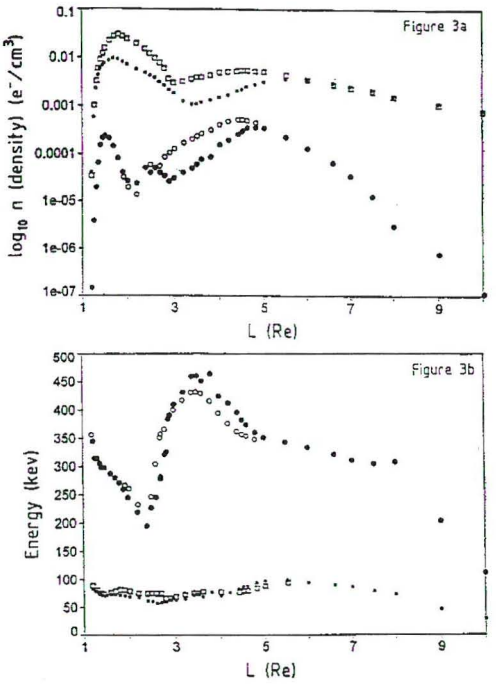

Figure 5: Equatorial distributions (L in Earth radii) of the densities (in e^-/cm^3) and characteristic energies (or temperatures in keV) of the two maxwellian velocity distribution functions that best fit the energy spectra of the relativistic electrons in the AE-8-MAX radiation belt models (Pierrard and Lemaire, 1996).

OERSTED observations

In cooperation with the Institut d'Aéronomie Spatiale de Belgique, the team of the Centre for Space Radiations, at the Université catholique de Louvain (UCL), has analysed the data of a Charged Particle Detector (CPD) along 3052 orbits of the Danish OERSTED satellite. The CPD instrument has been developed by P. Stauning of the Danish Meteorological Institute. The CPD detects the flux of the protons (E > 0.2 MeV) and electrons (E > 30 keV) in two orthogonal directions.

Software calibrations of the detectors composing this experiment have been performed at UCL using the GEANT software developed at CERN. The results of this Monte Carlo simulation have been compared to the hardware calibration of this instrument. The results are reported in a Technical Report prepared by Cyamukungu *et al.* (1997). Preliminary results based on the three first months of observations are shown in figure 6.

This figure illustrates on a world map the difference (CP2 – CP1)/CP1 in the count rate of the CP1 and CP2 particle detectors measuring the relative fluxes in two orthogonal directions for electrons above an energy threshold of 30 keV and protons of energies above 200 keV. This figure shows that the energetic proton fluxes measured at low altitude (400 km) in the South Atlantic Anomaly (near – 30° longitude) are highly anisotropic. Indeed, at low altitude most trapped particles are close to their mirror points and have a pitch angle distribution sharply peaked in the direction perpendicular to the magnetic field. In the future we will process the whole data sets collected by OERSTED and study Space Weather effects of solar activity and geomagnetic activity on the distribution of count/rates and fluxes collected during this ongoing mission. Preliminary results have been presented 2-4 May, 2000 at the Science Working Team meeting of the OERSTED mission in Grasse, France. They are reported in two publications: Cyamukungu *et al.* (2000), Stauning et al. (2000) and the Final Report of this PRODEX contract by Cyamukungu *et al.* (2001).

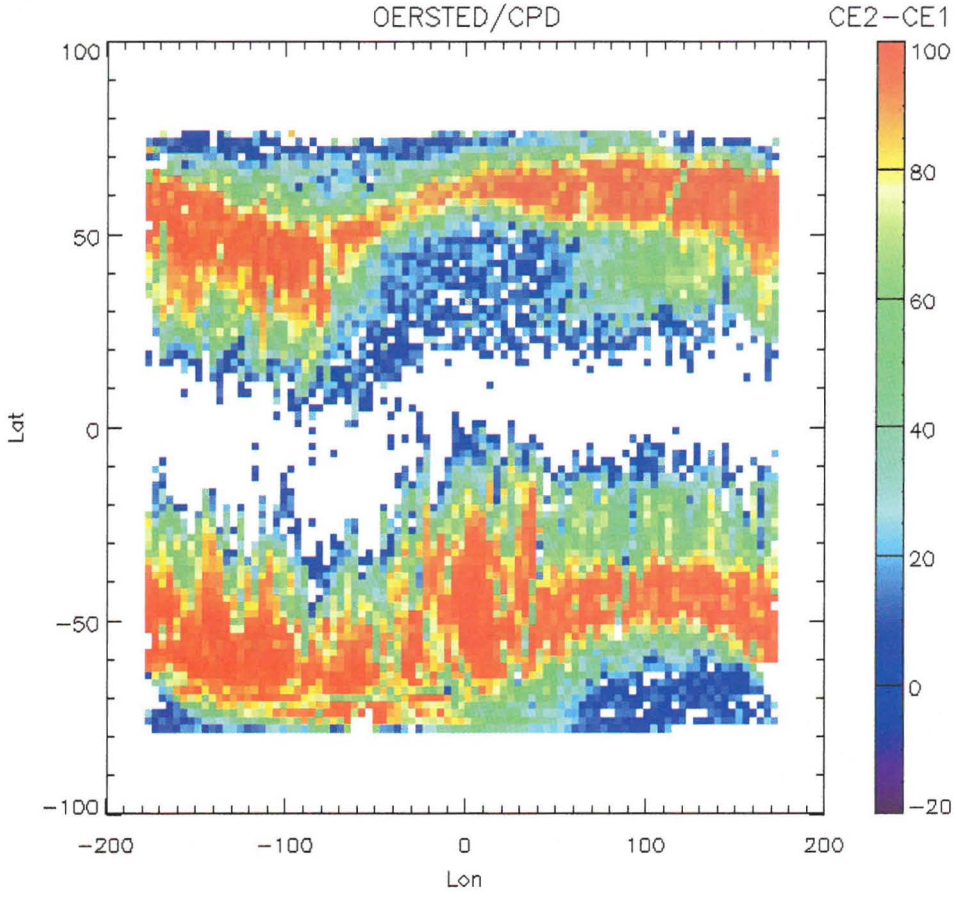

Figure 6: World map of the anisotropy of the electron flux measured in two perpendicular directions with the Charged Particle Detectors of the OERSTED satellite. The color code shows the ratio (CE2-CE1)/CE1 where CE1 and CE2 are the count rates of two detectors oriented at right angle from each other (Cyamukungu et al., 2000a).

"The data on which this study is based were obtained during the Space Mission and with the Experiment which are both briefly described in Appendix 1. Relevant Internet URL addresses are given when available".

EQUATOR-S observations

Three Scintillating Fibre Detectors (SFD) have been part of the German EQUATOR-S payload. This instrument was developed by L. Adams, QDA, ESTEC and constructed by SENSIS, Noordwijk. Software calibrations of these detectors for high energy electrons and protons have been performed at UCL with the GEANT code. They have been compared with hardware calibrations performed at PSI, Switzerland (Lemaire *et al.*, 1997).

The data collected by these instruments have been analysed by the research team of CSR at UCL, in cooperation with BIRA-IASB. Since the EQUATOR-S mission was on a GTO orbit, the SFD detectors traversed the centers of the inner and outer radiation belts twice every 14 hours. The omnidirectional flux of particles is proportional to the output current of the scintillating fibre readout. It varies as a function of time over the whole mission until the satellite was lost due to an unrecoverable failure following a massive injection of energetic particles deep into the magnetosphere. This occurred during severe geomagnetic storm activity. The enhanced activity toward the end of the EQUATOR-S mission is clearly illustrated in figure 7. The large geomagnetic variations of the Dst index shown in the bottom panel coincide with large injections of charged particle over a wide range of drift shells: it is associated with enhancements of the

Ring Current. The results of the analysis of the data from SFD-EQUATOR-S have been published by Cyamukungu et al. (1999).

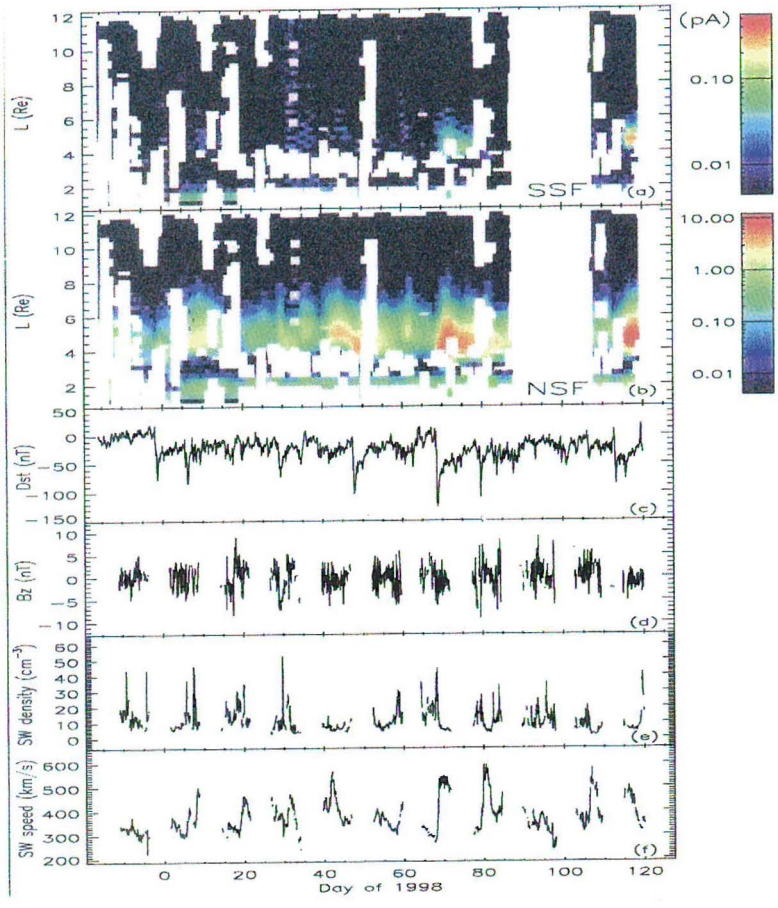

Figure 7: Equatorial distribution of the output currents of the SSF and NSF Scintillating Fibre Detectors on board of the EQUATORS-S spacecraft (panels a & b). Vertical scale is the equatorial distance in Earth radii; the horizontal axis is the Universal Time in days. Panels c, d, d and f illustrate respectively the geomagnetic activity index, D_{st} in nano-teslas, the northward component of the interplanetary magnetic field, B_Z, in nano-tesla, the solar wind density, in cm^{-3}, and bulk speed, in km/s. Large injections of energetic protons and electrons deep into the magnetosphere (seen in the panels a & b) coincide with large depressions in the D_{st} geomagnetic activity index (Cyamukungu et al., 1999).

"The data on which this study is based were obtained during the Space Mission and with the Experiment which are both briefly described in Appendix 1. Relevant Internet URL addresses are given when available".

SAMPEX observations

At the Workshop on "Radiation Belts: models and standards" convened, 17-20 October, 1995, in Brussels, at the Belgian Institute for Space Aeronomy, by J. Lemaire, IASB and M. Panasyuk, SINP, Moscow State University, the Belgian research team TREND under ESA contract has been offered by J.B. Blake, Aerospace Corporation, California, to access the "Proton/Electron Telescope" (PET) data collected during the ongoing SAMPEX American satellite mission. This instrument had been designed to develop a new low altitude empirical model for the trapped radiation belt protons between 20 and 500 MeV (Heynderickx *et al.*, 1999).
Global average models are obtained by binning and averaging the flux measurements over extended periods of time. It is implicitly assumed that the radiation environment which is surveyed remains unchanged over

the whole period of sampling. This is a "null hypothesis" that we wanted to test from a statistical point of view, by verifying whether the histograms of counts in a series of bins are indeed distributed according to a simple Poisson distributions. This statistical study has been reported by Pierrard *et al.* (2000). It showed that the observed departures from Poisson distributions of the PET/SAMPEX count rates in certain energy ranges can be attributed either to variations of the environment during sampling, or to the non-constancy of the detectors livetimes in regions where they are rapidly saturated due to extremely large fluxes of particles in the environment.

"The data on which this study is based were obtained during the Space Mission and with the Experiment which are both briefly described in Appendix 1. Relevant Internet URL addresses are given when available".

LIULIN observations

Dose and flux measurements collected on board of the Russian MIR station by the Bulgarian LIULIN dosimeter and fluxmeter have been analysed during the Belgo-Bulgarian bilateral cooperation project supported by SSTC research contract BL/10/B07. A database containing the observations for the years 1991 to 1993 have been built and stored at IASB-BIRA. An Atlas of monthly average dose and flux maps have been produced and analysed (Dachev et al., 1997a, 1997b, 1998; Lemaire and Dachev, 1998). Figure 8 shows world maps of 1) the number of observations per geographical bins at the altitude of the MIR station (top panel), 2) of the monthly average fluxes of particles above the LIULIN's energy thresholds (mid panel), as well as 3) of the monthly average doses deposited in the detectors as a function of geographical longitudes and latitudes. This plot corresponds to averages over 28 days during the month of January 1991.

The graphical plotting subroutine used to produce figure 8 has been developed in 1988 by V. Bashkirov, MSU, while he visited the Belgian Institute for Space Aeronomy for a period of 6 months. The originality of the graphical tools is to adapt the bin size to the number of measurements available in these bins (Bashkirov, 1998).

It can be seen that the measured fluxes and doses have broad peaks in the region of the South Atlantic magnetic field anomaly where the geomagnetic field has a characteristic minimum. This region is where Low Earth Orbiting (LEO) satellites experience most often Single Event Upsets (SEU). This bilateral Belgo-Bulgarian study contributes new results for the International Space Weather program, especially by demonstrating that new energetic ring current particles are first injected in the equatorial region of the radiation belts; it takes several days before their pitch angles is scattered into the loss cone, i.e. before they are eventually observed at the low altitude of the MIR space station, and precipitated in the atmosphere of the Earth.

The formation of new radiation belts in the slot region has also been observed at low altitude during geomagnetically disturbed periods with the LIULIN detector (Dachev et al. 2000). The distribution of binned/average fluxes and doses observed around the peak value in the SAA has been fitted by an analytical surface with x being the longitude, y the latitude and z the flux or dose measurements. The value of z_{max}, the fitted peak value, as well as its geographical position (x_{max}, y_{max}) depend on the altitude of MIR and on the levels of geomagnetic activity. This has been demonstrated in a paper by Dachev et al. (1999).

The study of Space Weather effect using the LIULIN data as well as those of the CPD onboard of OERSTED are not yet finished and will be continued in 2001. An extended data set should be collected on the International Space Station (ISS) with the new LIULIN-4 detector. This new detector has been calibrated using the GEANT code at UCL. Similar calculations have been performed at UCL for the CPD and SFD instruments mentioned above. The new LIULIN-4 detector has also been calibrated within a proton beam at the Cyclotron of the Université catholique de Louvain (UCL). The results of this calibration are reported in the Technical Note by Schmitz *et al.* (1999) and were presented in September 2000 at the international RADECS 2000 conference in Louvain-La-Neuve Cyamukungu *et al.* (2000b).

A novel method of characterizing the dependence of the angular response of a detector as a function of energy has been identified and developed at the Center for Space Radiations of UCL. Instead of assuming this efficiency to be a separable function of the energy and of the angle of incidence, the efficiency is now

determined as a non-linear function of both independent variables (i.e. energy and angle of incidence of the particles beam).

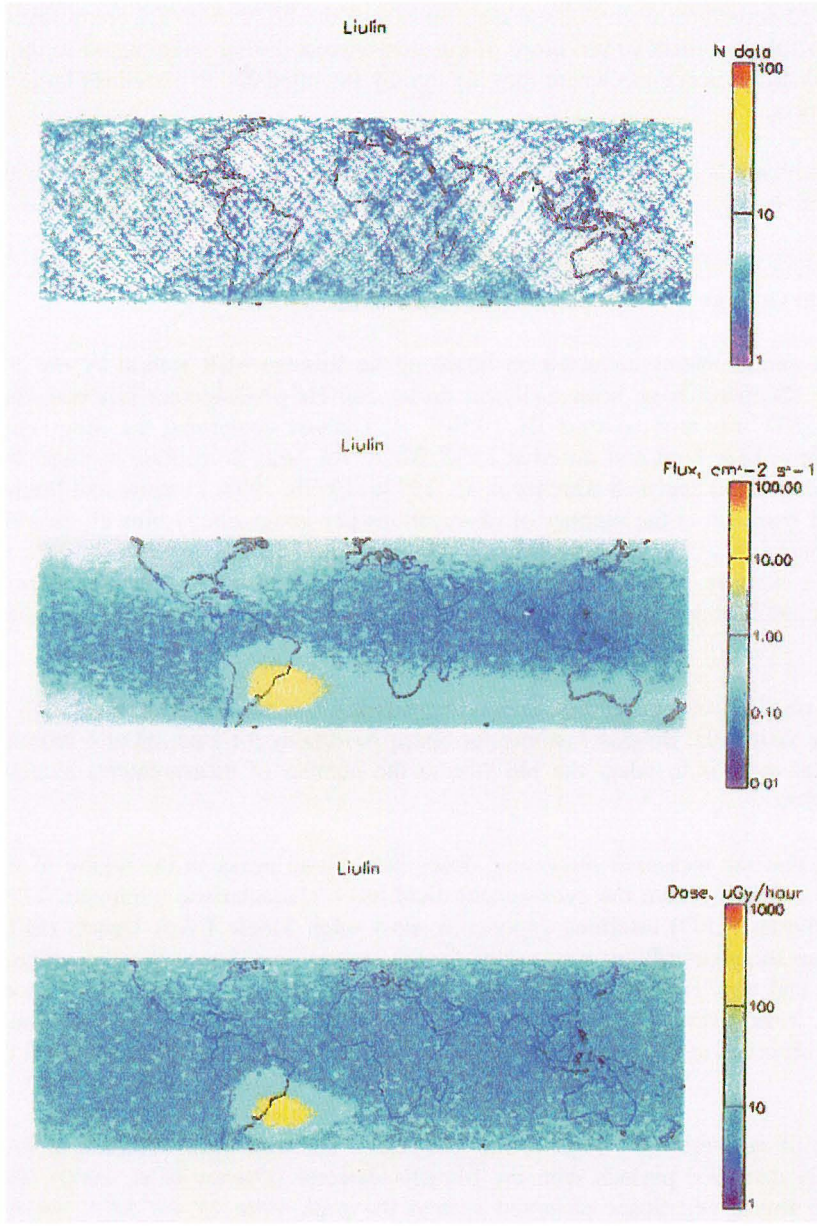

Figure 8: World maps of distribution of fluxes (in particles/cm^2/s; mid panel); doses (in μ Gy/hour; bottom panel), and number of measurements (per bins) collected by the LIULIN dosimeter-fluxmeter on board of the Russian MIR station over the month of January 1991. The peaks of the Earth observed in the fluxes and doses over the region of the South Atlantic Anomaly are due to the deeper penetration of the drift shells of trapped particles in this region of the Earth where the geomagnetic field intensity has a depressed intensity (Dachev et al., 1998).

"The data on which this study is based were obtained during the Space Mission and with the Experiment which are both briefly described in Appendix 1. Relevant Internet URL addresses are given when available".

CONCLUSIONS

This article summarizes the main results obtained by the authors at BIRA-IASB and at the Center for Space Radiation at UCL in projects that were supported by ESA contracts, by PRODEX-OERSTED and by bilateral agreements between Belgium and Bulgaria. This review covered exclusively the fields of

1. plasmaspheric models and convective stability,
2. impulsive penetration of solar wind-magnetosheath into the magnetosphere,
3. observations of energetic charged particles in the magnetosphere. Besides analysing the observations of the OERSTED, EQUATOR-S and LIULIN detectors, the LIULIN-4 that will operate on board of the ISS has also been calibrated in a proton beam at the cyclotron of UCL.

In the future we plan to use the data sets of these missions to improve our understanding of the influence of the changing solar wind on the magnetosphere and especially on the plasmasphere, atmosphere and radiation belts.

APPENDIX 1: INFORMATION CONCERNING THE SPACE MISSIONS AND EXPERIMENTS MENTIONED IN THIS CONTRIBUTION

Some of the work reported in this contribution is of theoretical order or numerical modelling of the density distribution in the plasmasphere, and is therefore not linked nor associated with any particular mission or any experimental observations.

But plasma data from different space instruments (CPD, SFD, PET, LIULIN) have also been analysed at BIRA-IASB and at the Institute for Nuclear Physics of UCL; The space missions (OERSTED, EQUATOR-S, SAMPEX, MIR) to which these instruments belong to will be briefly outlined below. Other space missions that the Plasma Group at BIRA-IASB was also concerned with (ULYSSE, CLUSTER, INTERBALL) have been reported elsewhere in this volume, and will not be repeated here.

- **The Charged Particle Telescope (CPD) is part of the OERSTED mission.**

The OERSTED spacecraft was launched February 23, 1999, into a near-polar (96.5 deg) low altitude (849 km x 613 km) orbit. Provisionally collection of data is planned for a period of 14 months. The measurements shall be used to improve the existing models of the Earth's magnetic field and to determine the changes of the field. http://web.dmi.dk/projects/oersted/
The CPD Particle detector to measure the flux of energetic electrons (30 keV), protons (E>200 MeV), and alpha particles (E>1 MeV). The instrument is built at the Danish Meteorological Institute. http://www.fynu.ucl.ac.be/users/m.cyamukungu/oersted/shortrep.html

- **The Scintilation Fibre Detector (SFD) is part of the EQUATOR-S mission**

The EQUATOR-S was a low-cost mission designed to study the Earth's equatorial magnetosphere out to distances of 67300 km . Unique features of EQUATOR-S are its nearly equatorial orbit and its high spin rate. It was launched as an auxiliary payload on an Ariane-4 on December 2nd, 1997. The mission terminated in May 1998 due to an unrecoverd failure after a catastrophic magnetic storm injection of energetic particles into the magnetosphere.
http://www.mpe-garching.mpg.de/www_plas/EQS/eq-s-home.html
The SFD experiment is based on the light emission property of some materials when hit by ionising radiation. Optical fibers guide the emitted light to a photodiode operated in current mode. A logarithmic amplifier converts this detector current to an analog output voltage. Energy discrimination is achieved by using three differently shielded channels. This way electrons above 0.4 and 2 MeV are measured, and protons above 8.6 and 30 MeV, with a time resolution of 64 s. A constant current is added periodically to calibrate the system.

- **The Proton Electron Telescope (PET) is part of the SAMPEX mission**

The Solar Anomalous and Magnetospheric Particle Explorer (SAMPEX) is the first of a series of spacecraft that was launched under the Small Explorer (SMEX) mission of low cost spacecraft. The main objectives of SAMPEX experiments was to obtain data for several continuous years on the anomalous, components of cosmic rays, on energetic particle emissions from the sun, and on the precipitating magnetospheric relativistic electrons. It carries four science instruments: (1) low energy ion composition analyzer (LICA); (2) heavy ion large telescope (HILT); (3) mass spectrometer telescope (MAST); and (4) proton electron telescope (PET). For more details, see IEEE Transactions on Geoscience and Remote Sensing, Vol 31, May 1993, pages 531-541.
http://nssdc.gsfc.nasa.gov/space/

The PET consists of an array of eight, lithium-drifted solid state detectors, together covering the energy range of 1--30 MeV for electrons, 18--85 Mev/nucleon for H and He, and 54-195 MeV/nucleon for the heavier elements.
http://www.magnet.oma.be/trend4/public/trend3/cha05.pdf

- **The LIULIN dosimeter-Radiometer has operated onboard of the MIR station and a updated version will be flown in 2001 on the International Space Station (ISS)**

The MIR station was a Russian orbital laboratory in LEO at an altitude of 300-450 km. It was in orbit for over 14 years. The first element of the station was launched on February 20, 1986. It traversed every day several times the South Atlantic Anomaly (SAA) where the Radiation Belts have their deepest point of penetration in the Earth atmosphere. This is the place where most of the low altitude satellite with a high inclination angle experience the largest rate of Single Event Upsets (SEU) due to the bombarment of the spacecraft , by energetic Van Allen Belt particles. http://www.hq.nasa.gov/osf/mir/

The main purpose of the LIULIN-4 detector is to monitor simultaneously the doses and fluxes at 4 separate locations. But it can also be used for personnel dosimetry. The main contribution to the count rate measured by LIULIN is due to protons and electrons that have energy respectively higher than 100 MeV and 10 MeV outside MIR space station. LIULIN measurements were carried out under a wide variety of solar and geomagnetic activity conditions. They provide an excellent opportunity to study effects on the dose-rates and fluxes in the near Earth radiation environment over long time periods,
as well as rapid changes, induced by solar proton events and geomagnetic disturbances.
http://www.fynu.ucl.ac.be/themes/he/radiations.html

REFERENCES

Bashkirov, V., Gridplot: Idl Package For Binning And Mapping Unevenly Distributed Data Sets: With Application To The Liulin Flux And Dose Measurements, Technical Notes, Iasb, Brussels, July 1998.

Beliaev, A.A. And Lemaire, J.F., Evaluation Of The Inp Radiation Belts Models, Technical Note A, Estec/Contract 9828/92/Nl/Fm, Aeronomica Acta A, June 12, 1994.

Beliaev, A.A. And Lemaire, J.F., Comparison Between Nasa And Inp/Msu Radiation Belt Models, In "Radiation Belts: Models And Standards, Eds. J.F. Lemaire, D. Heynderickx And D.B. Baker, Agu Geophys. Monograph 97, P. 141-145, 1996.

Carpenter, D.L. And Anderson, R.R., An Isee/Whistler Model Of Equatorial Electron Density In The Magnetosphere, J. Geophys. Res., 97, 1097-1108, 1992.

Comfort, R.H., Thermal Structure Of The Plasmasphere, Advanced In Space Research, 17, (10) 175-184, 1996.

Comfort, R.H., Waite, Jr., J.H. And Chappell, C.R., Thermal Ion Temperatures From The Retarding Ion Mass Spectrometer On De-1, Journal Of Geophysical Research, 90, 3475-86, 1985.

Cyamukungu, M., Grégoire, Gh., Lemaire, J. And Stauning, P., The Charged Particle Detector (Cpd) On The Oersted Satellite: Description And Evaluation, Belgian Institute For Space Aeronomy, Technical Report A, Brussels, 1997.

Cyamukungu, M., Grégoire, Gh., Stauning, P. And Lemaire, J., The Charged Particle Detector (Cpd): Data Analysis Methodology, In: Neubert, T. And Ultré-Guérard, P. (Eds.), Proceedings 3rd International Team Meeting Oersted, Grasse, France 2-4 May, 2000a.

Cyamukungu, M., Grégoire, Gh., Lemaire, J., Schmitz, H., In-Beam And Numerical Characterization Of Space Radiation Detector, Proceedings Of Radecs 2000, Lln, Sept. 2000b.

Cyamukungu, M., Grégoire, Gh., Heynderickx, D., Kruglanski, M., Blake, J.B., Selesnick, R. And Lemaire, J., Proton Spectra Detected By The Proton Switch (Ps) Onboard The Crres Satellite (Submitted 2001).

Cyamukungu, M., Lippens, C., Adams, L., Nickson R., Boeder, C., Pierrard, V., Daly, E., Grégoire, Gh. And Lemaire, J., Magnetic Storm Acceleration Of Radiation Belt Electrons Observed By The Scintillating Fibre Detector (Sfd) Onboard Equator-S, Ann. Geophys., 17, 1622-1625, 1999.

Dachev, Ts. P., Tomov, B.T., Matviichuk, Yu.N., Koleva, R.T., Semkova, J.V., Petrov, V.V., Ivanov, Yu.I., Shurshakov, V.A., Lemaire, J., Study Of Dose Rate And Flux Distribution After Solar Proton Events In 1989-1994 Time Interval, Proc. Of The 4th National Conference On Solar-Terrestrial Influences, 11, Sofia, October 1997a.

Dachev, Ts. P., Tomov, B.T., Matviichuk, Yu.N., Koleva, R.T., Semkova, J.V., Petrov, V.V., Ivanov, Yu.I., Shurshakov, V.A., Lemaire, J., Long Term Variations Of Mir Radiation Environment As Observed By The Liulin Dosimeter, Proc. Of The 4th National Conference On Solar-Terrestrial Influences, 9, Sofia, October 1997b.

Dachev, Ts. P., Lemaire J.F., Tomov, B.T., Matviichuk, Yu., Koleva, R.T., Semkova, J.V., Petrov, J.V., And Shurskakov, V.A., Overview Of The Inner Magnetosphere Observed By The Liulin Instrument On The Mir Space Station, In Proceedings Of The "First International Conference On Astronomy And Space Sciences, Mafracq, Al Al-Bayt University, 4-6 May, 1998 (Eds. Hamid Mk), 1999.

Dachev, Ts. P., Tomov, B., Matviichuk, Yu., Lemaire, J. Grégoire, Gh., Cyamukungu, M., Schmitz, H., Spurny, K.F., Calibration Results Obtained With Liulin-4 Type Dosimeters, Submitted To Advanced Space Research, 2000.

Echim, M.M. And Lemaire, J.F., Laboratory And Numerical Simulations Of The Impulsive Penetration Mechanism, Space Science Reviews, 92, 565-601, 2000.

Gringauz, K.I. And Bezrukikh, V.B., Asymmetry Of The Earth's Plasmasphere In The Direction Noon-Midnight From Prognoz-1 And Prognoz-2 Data, Journal Of Atmospheric And Terrestrial Physics, 38, 1071-6, 1976.

Gringauz, K.I., Structure And Properties Of The Earth's Plasmasphere, Advances In Space Research, 5(4), 391-400, 1985.

Heynderickx, D., Kruglanski, M., Pierrard, V., Lemaire, J., Looper, M.D., And Blake, J.B., A Low Altitude Trapped Proton Model For Solar Minimum Conditions Based On Sampex/Pet Data, Ieee.Transactions On Nuclear Science, 46(6), 1475-1480, 1999.

Horwitz, J.L., Blanc, M., Daglis, I., Lemaire, J.F., Moldwin, M.B., Orsini, S., Thorne, R.M., Watanabe, S., And Wolf, R.A., Source And Loss Processes In The Inner Magnetosphere, Chapter 4, In The Book: "Source And Loss Processes Of Magnetospheric Plasma", Issi Publication, Kluwer Academic Publishers, 1999.

Kozyra, J.U., Shelley, E.G., Comfort, R.H., Brace, L.H., Cravens, T.E. And Nagy, A.F., The Role Of Ring Current O^+ In The Formation Of Stable Auroral Red Arcs, Journal Of Geophysical Research, 92, 7487-502, 1987.

Lemaire, J. And Dachev, Ts., Final Report Of Joint Bulgarian-Belgian Research Project On The" Development Of Experimental Tests Of The Models Of The Earth's Radiation Environment On The Base Of Data Obtained By Liulin Instrument On Mir Space Station", 1998.

Lemaire, J. And Roth, M., Penetration Of Solar Wind Plasma Elements Into The Magnetosphere, J. Atmos. Terr. Phys., 40, 331-335, 1978.

Lemaire, J. And Roth, M., Non Steady-State Solar Wind – Magnetosphere Interaction, Space Science Reviews, 57, 59-108, 1991.

Lemaire, J., Gringauz, K.I., With Contribution By Carpenter, D.L. And Bassolo, V., The Earth's Plasmasphere, Book Published By Cambridge University Press, Isbn, 0.521.43091.7, 346 Pp., 1998.

Lemaire, J., Impulsive Penetration Of Filamentary Plasma Elements Into The Magnetospheres Of The Earth And Jupiter, Planet. Space Sci., 25, 887-890, 1977.

Lemaire, J., Hydrostatic Equilibrium And Convective Stability In The Plasmasphere, Journal Of Atmospheric And Solar-Terrestrial Physics, 61, 867-878, 1999.

Lemaire, J.F., The Formation Of Plasmaspheric Tails, Phys. Chem. Earth ©, Vol. 25, No 1-2, P. 9-17, 2000.

Lemaire, J., The Formation Of The Light-Ion-Trough And Peeling Off The Plasmasphere, Journal Of Atmospheric And Solar Terrestrial Physics, 63, 2001.

Lemaire, J., Lippens, C., Pierrard, V., Cyamukungu, M. And Grégoire, Gh., The Scintillating Fibre Detector (Sfd), Technical Note A, Iasb & Nuclear Physics Institute Ucl, 1997.

Newcomb, W.A., Convective Instability Induced By Gravity In A Plasma With A Frozen-In Magnetic Field, Physics Of Fluids, 4, 391-396, 1961.

Pierrard, V. And Lemaire, J., Fitting The Ae-8 Energy Spectra With Two Maxwellian Functions, Radiation Measurements, 26(3), 333-337, 1996a.

Pierrard, V. And Lemaire, J., Lorentzian Ion-Exosphere Model, Journal Of Geophysical Research, 101, 7923-7934, 1996b.

Pierrard, V. And Lemaire, J., Corrections To The Lorentzian Ion Exosphere Model, Journal Of Geophysical Research, 103, 4117, 1998.

Pierrard, V., Lemaire, J., Heynderickx, D., Kruglanski, M., Looper, M., Blake, J.B. And Mewaldt, D., Statistical Analysis Of Sampex Pet Proton Measurements, Nuclear Instruments And Methods In Physics Research A, 449, 378-382, 2000.

Pierrard, V. And Lemaire, J., Exospheric Model Of The Plasmasphere, J. Of Atmospheric And Solar-Terrestrial Physics, 63, 2001.

Reynolds, M.A., Ganguli, G., Lemaire, J., Fedder, J.A., Meier, R.R., And Melendez-Alvira, D.J., Thermal Plasmaspheric Morphology: Effect Of Geomagnetic And Solar Activity, J. Geophys. Res., 104, 10285-10294, 1999.

Schmitz, H., Cyamukungu, M., Dachev, Ts. And Grégoire, Gh., Calibration Of The Liulin-4 Dosimeter, Technical Notes, Ucl, 1999.

Scudder, J.D., On The Causes Of Temperature Change In Inhomogeneous Low-Density Astrophysical Plasmas, Astrophysical Journal, 398, 299-318, 1992a.

Scudder, J.D, Why All Stars Should Possess Circumstellar Temperature Inversions, Astrophysical Journal, 398, 319-49, 1992b.

Stauning, P., Davidson, P. And Cyamukungu, Oersted Cpd High-Energy Particle Observations And Radiation Effects In Satellite Instruments And Systems, In Neubert, T. And Ultré-Gérard, P. (Eds.): Proceedings Of The 3rd International Science Oersted Team Meeting, May 2-4, 2000, Grasse, France, 2000.

BIBLIOGRAPHY

Lemaire, J. & Schunk, R.W., Plasmaspheric Convection With Non-Closed Streamlines. *J. Atmosph.Terrest. Physics,* 56, 1629-1633, 1994.

De Keyser, J., Roth, M., Lemaire, J., Tsurutani, B.T., Ho, C.M. & Hammond, C.M., Theoretical Plasma Distributions Consistent With Ulysses Magnetic Field Observations In A Solar Wind Tangential Discontinuity, *Solar Physics*, 166, 415-422, 1996.

Daly, E.J., Lemaire, J., Heynderickx, D. & Rodgers, D.J., Problems With Models Of The Radiation Belts, *Ieee Transactions On Nuclear Science,* 43, No 2, 403-415, 1996.

Pierrard, V. & Lemaire, J.F., Lorentzian Ion-Exosphere Model , *Journal Of Geophysical Research*, 101, 7923-7934, 1996.

Baker, D.N., Lemaire, J.F. & Panasyuk, M.I., Researchers Chart Course For Updating Radiation Belt Models, *Eos, Trans. Agu,* 77, 23, 217-218, 1996.

Meuris, P., Meyer-Vernet, N. & Lemaire, J., The Detection Of Dust Grains By A Wire Dipole Antenna : The Radio Dust Analyser, *Journ. Geophys. Res.,* 101, 24471-24477, 1996.

Heynderickx, D., Kruglanski, M., Lemaire, J., Daly, E.J. & Evans, H.D.R., The Trapped Radiation Software Package Unirad, In *Radiation Belts: Models And Standards*, *Geophysical Monograph* 97, *Agu*, Lemaire, J.F., Heynderickx, D. And Baker, D.N. (Eds.), 305-309, 1996.

Beliaev, A.A. & Lemaire, J., Comparison Between Nasa And Inp/Msu Radiation Belt Models, In *Radiation Belts: Models And Standards*, *Geophysical Monograph* 97, *Agu*, Lemaire, J.F., Heynderickx, D. And Baker, D.N. (Eds.) 141-145, 1996.

Heynderickx, D., Kruglanski, M., Lemaire, J.F. & Daly, E.J., A New Tool For Calculating Drift Shell Averaged Atmospheric Density, Pp. 173-178, In *Radiation Belts: Models And Standards*, *Geophysical Monograph 97*, *Agu*, Lemaire, J.F., Heynderickx, D. And Baker, D.N. (Eds.), 173-178, 1996.

Heynderickx, D., Lemaire, J., Daly, E.J. & Evans, H.D.R., Calculating Low-Altitude Trapped Particle Fluxes With The Nasa Models Ap-8 And Ae-8, *Radiation Measurements*, 26(6), 947-952, 1996.

Lemaire, J.F., Heynderickx, D. & Baker, D.N. (Eds.), Radiation Belts: Models And Standards, *Geophysical Monograph 97*, *Agu*, (Isbn-087590-079-8), 1996.

Pierrard, V. & Lemaire, J., Fitting The Ae-8 Energy Spectra With Two Maxwellian Functions, Aeronomica Acta A N° 383, 1994, *Radiation Measurements,* 26, No 3, 333-337, 1996.

Verigin, M., Apathy, I., Kotova, G., Lemaire, J., Remizov, A., Rosenbauer, H., Sezgo, K., Slavin, J., Tatrallyay, M., Schwingenschuh, K. & Shutte, N., Dependence Of Martian Magnetopause Shape And Its Dimensions On Solar Wind Dynamic Pressure According To Phobos-2 Data (Rus), *Kosmicheskie Isslevovaniya*, 34, 595-603, 1996. Translated In Cosmic Research, 34, 551-558, 1996.

Maksimovic, M., Pierrard, V. & Lemaire, J.F., A Kinetic Model Of The Solar Wind With "Kappa" Distribution Functions In The Corona, *Astron. Astrophys.,* 324, 725-734, 1997.

Afonin, V.V., Bassolo, V.S., Smilauer, J. & Lemaire, J., Motion And Erosion Of The Night Side Plasmapause Region And Of The Associated Subauroral Electron Temperature Enhancement: Cosmos-900 Observations, *J. Geophys. Res.*, 102, 2093-2103, 1997.

Kotova, G., Verigin, M., Remizov, A., Shutte, N., Rosenbauer, H., Livi, S., Szego, K., Tatrallyay, M., Slavin, J., Lemaire, J., Schwingenschuh, K. & Zhang, T.-L., Study Of The Solar Wind Deceleration Upstream Of The Martian Terminator Bow Shock, *Journal Of Geophysical Research*, 102, 2165-2173, 1997.

Verigin, M., Kotova, G., Shutte, N., Remizov, A., Szegö, K., Tatrallyay, M., Apathy, I., Rosenbauer, H., Livi, S., Schwingenschuh, K., Slavin, J., Lemaire, J.F., Richter, A.K. & Zhang, T.-L., Quantitative Model Of The Martian Magnetopause Shape And Its Variation With The Solar Wind Ram Pressure Based On Phobos 2 Observations, *Journal Of Geophysical Research*, 102, 2147-2155, 1997.

Lemaire, J., & Gringauz, K.I., The Earth's Plasmasphere, *Cambridge University Press, Cambridge (Isbn 0.521.43091.7),* 346 Pp., 1998.

Pierrard, V. & Lemaire, J., A Collisional Kinetic Model Of The Polar Wind, *Journal Of Geophysical Research*, 103, 11701-11709, 1998.

De Keyser, J., Roth, M. & Lemaire, J., The Magnetospheric Driver Of Subauroral Ion Drift, *Geophysical Research Letters*, 25, 1625-1628, 1998.

Pierrard, V. & Lemaire, J., Correction To Lorentzian Ion Exosphere Model, *Journal Of Geophysical Research*, 103, 4117, 1998.

Pierrard, V., Maksimovic, M. & Lemaire, J., Electronic Velocity Distribution Function From The Solar Wind To The Corona, *Journal Of Geophysical Research* 104, 17,021-17,032, 1999.

Dachev, Ts. P., Tomov, B.T., Matviichuk, Yu., Koleva, R.T., Semkova, J.V., Petrov, V.M., Benghun, V., Ivanov, Yu., Shurshakov V.A., & Lemaire, J., Detailed Study Of The Solar Proton Events And Their Effects On The Dose Rate And Flux Distribution Observed By Liulin Instrument On Mir Station, *Radiation Measurements*, 30, 317-325, 1999.

Dachev, Ts. P., Koleva, R.T., Semkova, V., Tomov, B.T., Matviichuk, Yu., Petrov, V.M., V. Benghin, V., Ivanov, Yu., Shurshkov, V.A., & Lemaire, J., Solar Cycle Variations Of Mir Radiation Environment As Observed By The Liulin Dosimeter, *Radiation Measurements,* 30, 269-274, 1999.

Reynolds, M.A., Ganguli, G., Fedder, J.A., Lemaire, J., Meier, R.R., & Melendez-Alvira, D.J., Thermal Plasmaspheric Morphology: Effect Of Geomagnetic And Solar Activity, *Journal Of Geophysical Research*, 104, 10,285-10,294, 1999.

Lemaire, J.F., Hydrostatic Equilibrium And Convective Stability In The Plasmasphere. *Journal Of Atmospheric And Solar-Terrestrial Physics*, 61, 867-878, 1999.

Cyamukungu, M., Lippens, C., Adams, L., Nickon, R., Boeder, C, Pierrard, V, Daly, E, Gregoire Gh., & Lemaire, J., Magnetic Storm Acceleration Of Radiation Belt Electrons Observed By Scintillating Fibre Detector (Sfd) Onboard Equator-S. *Ann. Geophysicae*, 17, 1622-1625, 1999.

Blanc, M., Horwitz, J.L., Blake, J.B., Daglis, I., Lemaire, J., Moldwin, M.B., Orsini, S., Thorne, R.M., And Wolf, R.A., Source And Loss Processes In The Inner Magnetosphere, *Space Sc. Rev.*, 88, 137-206, 1999.

Echim, M.E. & Lemaire, J.F., Laboratory And Numerical Simulations Of The Impulsive Penetration Mechanism, *Space Science Reviews*, 92, 565-601, 2000.

Pierrard, V., Lemaire, J., Heynderickx, D., Kruglanski, M., Looper, M., Blake, B. & Mewaldt, D., Statistical Analysis Of Sampex Pet Proton Measurements, *Nuclear Instruments And Methods In Physic Research A* 449(2000), 378-382, 2000.